

## Numerical Simulation of Self Consolidating Concrete Flow in L–box Test

**Parviz Ghoddousi, PhD**, Dept. of Civil Engineering, Iran University of Science and Technology, Iran

**Masoud Hosseinpoor, MSc**, Dept. of Civil Engineering, Iran University of Science and Technology, Iran

**Behrouz Esmaeilkhanian, BSc**, Dept. of Civil Engineering, Isfahan University of Technology, Iran

### ABSTRACT

*Self consolidating concrete (SCC) can be considered as a non-Newtonian fluid. There are several models describing the behavior of SCC such as Herschel-Bulkley or Bingham models. If one can determine the rheological parameters, yield stress and viscosity, of these models for a specific SCC mixture, the properties of fresh SCC such as flowability, fillingability and workability can then be predicted. It can be used in the field of full scale casting and molding of SCC.*

*Ordinary qualitative output that can be obtained from tests such as L-box, slump flow and V-funnel are also used in these fields. However, such output are not that much reliable since these tests are basically experimental. Besides, the results of such tests are not in good agreement namely the output can be in complete contradict for some cases. One reason to explain such disagreement is that the effect of rheological parameters is neglected in common methods of measuring tests output.*

*In this paper, SCC flow in L-box test is simulated with respect to dam-break phenomenon. Mass conservation and Navier-Stokes equations are solved using a numerical method. Rheological parameters of SCC can be obtained from the results of this simulation. Experimental results verify the derived equations.*

**Keywords:** Self consolidating concrete, Rheological parameters, L-box test, Nguyen et al. model, Dam-break phenomenon

## INTRODUCTION

Self-consolidating concrete (SCC) is defined as a concrete that has excellent deformability and high resistance to segregation, and can be filled in a heavy reinforced area without applying any vibration.<sup>1</sup> From a rheological point of view, a successful SCC is characterized by low yield value needed for high capacity of deformation, and moderate viscosity necessary to ensure uniform suspension of solid particles during casting and thereafter until the setting.<sup>2</sup>

The viscosity ( $\mu$ ) of a fluid may be defined as the ratio of shear stress to the shear strain ( $\gamma$ ). A fluid, whose viscosity ( $\mu$ ) does not change with the rate of deformation or shear strain ( $\gamma$ ), is known as a Newtonian fluid. If we draw a graph showing shear strain ( $\gamma$ ) at abscissa and stress as ordinate, we find that a Newtonian fluid will be represented by a straight line.

A fluid, whose viscosity ( $\mu$ ) changes with the rate of deformation of shear strain ( $\gamma$ ), is known as a non-Newtonian fluid. The non-Newtonian fluid will be represented by a curve.

The most common method used to determine yield stress ( $\tau_0$ ) is by extrapolating the stress-strain rate flow curve to zero strain through use of an appropriate model. The most widely used model is Bingham's linear approximation for flow of a viscoelastic material. But, at best, the Bingham model provides an estimate of yield stress ( $\tau_0$ ) at low solids concentrations and loses accuracy as the solids concentration increases. Other models more closely approximate the actual flow behavior of cement suspensions, including those of Herschel-Bulkley.<sup>3</sup> Both Bingham model and Herschel-Bulkley model are non-Newtonian flows.

Various empirical tests are proposed for evaluating the flowability, the passing ability and the segregation resistance of SCC. D'Aloid Schwartztruber et al.<sup>4</sup> reported that, rheological properties, i.e. viscosity ( $\mu$ ) and shear yield stress ( $\tau_0$ ), are well correlated with empirical test results in the range of flowable mixes. They have concluded that easier empirical tests can be performed instead of more complex rheological ones.

Several models are proposed to correlate rheological properties to the results of empirical tests.<sup>5,6</sup>

Nguyen et al.<sup>6</sup> have developed a theoretical model to correlate between L-box blocking ratio ( $\frac{H_2}{H_1}$ ) with the yield stress ( $\tau_0$ ), provided that the material stays homogeneous and the gate is slowly lifted. In order to minimize the inertia effects, they considered that the gate is slowly lifted. So that, the test results only could be depend on yield stress ( $\tau_0$ ).

The L-box test is one of the common test methods for SCC. It consists of two parts; the vertical part is filled with concrete. After the gate is lifted, the concrete can flow into the horizontal part.

Usually, vertical reinforcement bars are placed just after the gate so that concrete has to flow in between them.

The presence of the steel bars in L-box, leads to more complex analysis, base on this assumption, Nguyen et al.<sup>6</sup> removed bars for their theoretical analysis of the flow. But for the experimental quantification, the influence of the steel bars has been considered.

The objective of the present study is to propose a theoretical analysis for a non-Newtonian fluid flow base on dam-break theory. In the present paper by using the dam break phenomenon, the flow of a non Newtonian fluid during L-box test is analyzed considering a Bingham model for the shear stress of fluid. Finally, experimental data from L-box test and results of the theoretical model are compared and it is shown that this model predicts the yield stress of concrete more accurate than that proposed by Nguyen et al<sup>6</sup>.

### NGUYEN ET AL.<sup>6</sup> PROPOSED MODEL

In this paper assuming a very low velocity for the lifting of gate (a time of 10 seconds for the complete opening of gate), writers neglected the effects of inertia in the momentum equation. Therefore, it can be concluded that the exerted shear stress on the flow due to inertia varies in the form of a fraction of yield stress depending on the velocity of lifting. As a result, if the lifting velocity is low enough, the shear forces that are the effects of inertia are negligible making it possible to omit the effects of plastic viscosity.

In order to analyze the flow of concrete, authors used a volumetric element of fluid in the flume when the motion of SCC is arrested.

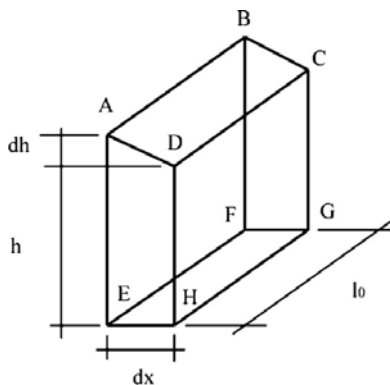


Fig.1 Volumetric Element of Concrete in the Arrested State

Equilibrium of forces acting on the element and conservation of mass equation results in:

$$L = \frac{h_0}{A} + \frac{l_0}{2A} \ln \left( \frac{l_0}{l_0 + 2h_0} \right) \quad (1)$$

Where  $L$  is the length of spread of concrete in the flume,  $h_0$  is the thickness of the deposit at  $x=0$ ,  $A = \frac{2\tau_0}{\rho g l_0}$ ,  $\rho$ ,  $g$  and  $l_0=20\text{cm}$  are the fluid density, gravity acceleration and flow width of L-box respectively.

In Eq. 1 it is assumed that spread length,  $L$ , is less than horizontal part length  $L_0$ . Another case also considered that  $L = L_0$ . In this case, the relation between the thicknesses ( $H_1$  at  $x=0$  and  $H_2$  at  $x=L_0$ ) of the deposit at the extreme sides of the box, was expressed as following equation.

$$L_0 = \frac{H_1 - H_2}{A} + \frac{l_0}{2A} \ln \left( \frac{l_0 + 2H_2}{l_0 + 2H_1} \right) \quad (2)$$

Furthermore, Nguyen et al.<sup>6</sup> have proposed the equation which can be used the ratio  $\frac{H_2}{H_1}$  if the yield stress is known.

$$4V' \frac{L-r}{L+r} - Ln \left( \frac{L+r+4V'}{L+r+4rV'} \right) = \frac{2AL_0}{l_0} \quad (3)$$

Eq. 3 is obtained from Eq. 2 by approximation of total volume sample  $V$  by  $l_0 L_0 (H_1 + H_2)/2$  and introducing  $r = \frac{H_2}{H_1}$  and dimensionless volume  $V' = V/(l_0^2 L_0)$ .

At last, the correlation between  $\frac{H_2}{H_1}$  ratio with the yield stress presented. The relationship is expressed as following equation.

$$H_1 - H_2 = \frac{\tau_0 L_0}{\rho g} \left( \frac{l_0 L_0}{V} + \frac{2}{l_0} \right) \cong 15 \frac{\tau_0}{\rho g} \quad (4)$$

Substituting  $H_{avg} = \frac{H_1 + H_2}{2} = \frac{V}{l_0 L_0}$  into Eq. 4 results:

$$\frac{H_2}{H_1} = \frac{2H_{avg} - (H_1 - H_2)}{2H_{avg} + (H_1 - H_2)} \cong \frac{\rho g - 84\tau_0}{\rho g + 84\tau_0} \quad (5)$$

Solving Eq. 5 for  $\tau_0$  gives:

$$\tau_0 \cong \frac{\rho g \left(1 - \frac{H_2}{H_1}\right)}{84 \left(1 + \frac{H_2}{H_1}\right)} \quad (6)$$

Their analysis is based on L-box which the volume of vertical part was 12.5 liters and the length of horizontal part was 0.70m. But more common L-box which is used in this study has different dimension, with 0.80m the length of horizontal part and 12 liters, the volume of vertical part.

Hence, substitution of new values in their model, obtains generalized version of Nguyen et al.<sup>6</sup> model as following equations.

Setting  $L_0=80$  cm and  $V=12$  lit in Eq. 3 gives:

$$H_1 - H_2 = \frac{\tau_0 L_0}{\rho g} \left( \frac{l_0 L_0}{V} + \frac{2}{l_0} \right) \cong 18.67 \frac{\tau_0}{\rho g} \quad (7)$$

Upon substituting  $H_{avg} = \frac{H_1 + H_2}{2} = \frac{V}{l_0 L_0}$  in Eq. 7 we have:

$$\frac{H_2}{H_1} = \frac{2H_{avg} - (H_1 - H_2)}{2H_{avg} + (H_1 - H_2)} \cong \frac{\rho g - 124.44\tau_0}{\rho g + 124.44\tau_0} \quad (8)$$

Solving Eq. 8 for  $\tau_0$  gives:

$$\tau_0 \cong \frac{\rho g \left(1 - \frac{H_2}{H_1}\right)}{124.44 \left(1 + \frac{H_2}{H_1}\right)} \quad (9)$$

## DAM-BREAK MODEL

Physical conditions of dam break phenomenon are so analogous to that of L-Box test. Sudden break of a dam which results in the release of a huge body of water into the downstream lands is called dam break. This unsteady flow of water is widely studied by hydraulics engineers because of its dangerous consequences. In addition to hydraulics, this phenomenon has been used in other fields of science or industry where the spread of a fluid needs to be controlled and monitored. Most of such fluids are non Newtonian and does not have known rheological properties just like concrete. It is proved that by controlling the mechanism of slumping of concrete in the slump test it is likely to measure the rheological properties of

fresh concrete.<sup>7</sup>

Since the mechanism of dam break is so close to what occurs in the L-Box test which is indeed a sudden opening of gate resulting in the flow of fresh SCC into the horizontal downstream flume, it is then possible to utilize the governing equations of dam break problems for non Newtonian fluids for the flow analysis of SCC in the L-box test.

The following assumptions are made.

- Flow of the fluid is on the horizontal plane.
- We set the coordinate system (x,z) so that x is aligned to the horizon and z is perpendicular to it where z=0 shows the bottom of flume.
- Velocity field is denoted by (u,w).

When assuming a laminar flow for the fluid, the dominant stresses are vertical shear stresses  $\tau_{xy}$ , and the shearing rate can be expressed by  $u_z = \frac{\partial u}{\partial z}$ . The rheological model can be summarized as below:

$$\tau_{xz} = \eta(u_z)u_z + \tau_y \operatorname{sgn}(u_z) \quad \text{if } |\tau_{xz}| \geq \tau_y \quad (10)$$

$$u_z = 0 \quad \text{if } |\tau_{xz}| < \tau_y \quad (11)$$

$$\eta(u_z) = K |u_z|^{n-1} \quad \text{non-linear viscosity} \quad (12)$$

where  $K_n$  is the ‘consistency’, n a power law index that governs the degree of shear thinning or thickening.

If the velocity of lifting is low, inertia can be neglected in Navier-Stokes equations. So these equations turn into the form:

$$0 = -\frac{\partial p}{\partial x} + \frac{\partial \tau_{xz}}{\partial z} \quad (13)$$

$$0 = -\frac{\partial p}{\partial z} - 1 \quad (14)$$

Mass conservation is in the form of:

$$\frac{\partial h}{\partial t} = -\frac{\partial q}{\partial x} \quad (15)$$

One solution for the above equation is<sup>8</sup>:

$$h_t = \left( \frac{\rho g}{K} \right)^{1/n} \frac{\partial}{\partial x} \left[ \frac{n |h_x|^{1/n-1} Y^{1+1/n}}{(n+1)(2n+1)} [(1+2n)h - nY] h_x \right] \quad (16)$$

Where Y is a boundary value for no-flux condition and is defined as following equation:

$$Y = h - \frac{\tau_0}{\rho g |h_x|} \quad \text{Where } \tau_y = \tau_0 \quad (17)$$

For a dam break problem of a column with height H and length L we have:

$$h = \begin{cases} H, & 0 \leq x \leq L \\ 0, & x > L. \end{cases} \quad (18)$$

#### DIMENSIONLESS FORMULATING

Upon defining the following dimensionless parameters we rewrite Eq. 16:

$$x = L\hat{x}, z = H\hat{z}, h = H\hat{h}, Y = H\hat{Y}, t = \frac{L}{H} \left( \frac{KL}{\rho g H^2} \right)^{1/n} \hat{t} \quad (19)$$

$$h_t = \frac{\partial}{\partial x} \left[ \frac{n |h_x|^{1/n-1} Y^{1+1/n}}{(n+1)(2n+1)} [(1+2n)h - nY] h_x \right] \quad (20)$$

$$Y = h - \frac{B}{|h_x|} \quad (21)$$

Where B is a dimensionless parameter and is called Bingham number:

$$B = \frac{\tau_0 L}{\rho g H^2} \quad (22)$$

And initial condition of problem becomes:

$$h(x) = \begin{cases} 1, & 0 \leq x \leq 1 \\ 0, & x > 1. \end{cases} \quad (23)$$

Conservation of mass turns into the form:

$$\int_0^{x_f} h dx = 1 \tag{24}$$

Along the same line with the model proposed by Nguyen et al.<sup>6</sup>, two cases can be considered here: first the case in which due to great values of yield stress ( $\tau_0$ ) all the initial column of fluid does not participate in flow. Consequently there is a point ( $x_{y\infty}$ ) behind which the fluid would not move. On the contrary, in the other one the entire initial step takes part in flow since its yield stress is smaller. In both cases, the front position of flow reaches a final point when the motion is arrested that we name it here  $x_{f\infty}$ <sup>8</sup>.

Since the values of  $\tau_0$  are relatively small for SCC, only the second case occurs in the L-box test.

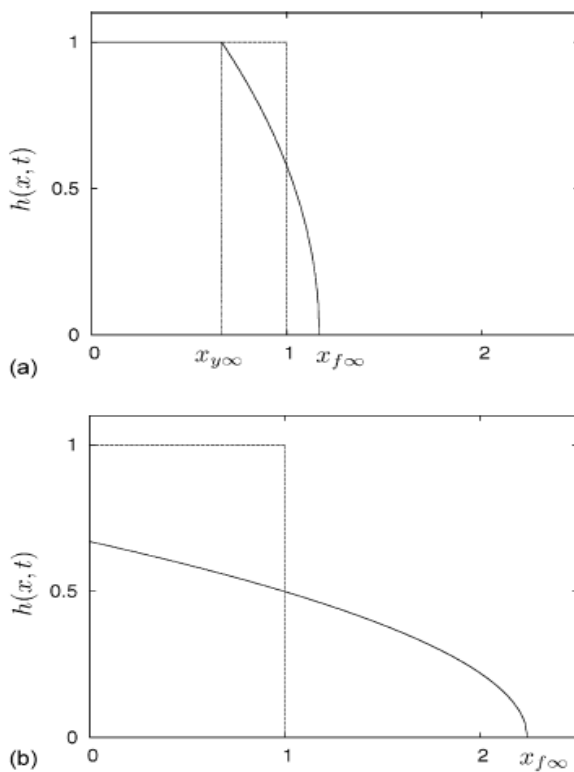


Fig.2 The Initial Profile of Fluid (Dashed Line) and Two Examples of Final Deposits (Solid Lines). If B Is Large Enough Not All of the Fluid Takes Part in the Motion and There Is a Discontinuity in the Gradient of the Final Height Profile as Shown in Fig (a). However, for Small Values of B All of the Fluid Flows and the Final Profile Will Be of the Form (b).

According to G.P. Matson et.al<sup>7</sup> and N.J. Balmforth et.al<sup>8</sup> in the case of small values of  $\tau_0$  which is more common for SCC it can be shown that if  $B < 1/3$ , ( $x_{y\infty} < 0$ ), the entire fluid flows in the flume. The profile of the final state of the fluid can then be expressed by:

$$h_{\infty}(x) = \sqrt{2B(x_{f\infty} - x)} \tag{25}$$

$$\text{And } x_{f\infty} = \left(\frac{9}{8B}\right)^{1/3} \quad (26)$$

Putting Eq. 26 into Eq. 25 gives:

$$h_{\infty}(x) = \sqrt{2B \left[ \left(\frac{9}{8B}\right)^{1/3} - x \right]} \quad (27)$$

Finally by simplifying Eq. 27 we have:

$$h_{\infty}(x) = \sqrt{(3B)^{2/3} - 2Bx} \quad (28)$$

Now, it is assumed that when the front position of flow reaches the end wall of L-box and the flow stops (the time when  $H_1$  and  $H_2$  are read in the L-Box test), the height of profile for every point along the flume is equal to that when there was no wall and the flow could continue until its motion was arrested due to the equilibrium of forces ( $h_{\infty}$ ). Hence at this time we have:

$$x = \frac{X}{L} = \frac{0}{0.1} \quad \text{at } x=0 \text{ cm}; \quad (29)$$

$$x = \frac{X}{L} = \frac{0.8}{0.1} = 8 \quad \text{at } x=80 \text{ cm}; \quad (30)$$

$$\frac{H_2}{H_1} = \frac{h_{\infty}(8)}{h_{\infty}(0)} = \frac{\sqrt{(3B)^{2/3} - 2B \times 8}}{\sqrt{(3B)^{2/3} - 2B \times 0}} \quad (31)$$

$$\frac{H_2}{H_1} = \frac{h_{\infty}(8)}{h_{\infty}(0)} = \frac{\sqrt{(3B)^{2/3} - 16B}}{\sqrt{(3B)^{2/3}}} = \sqrt{1 - \frac{16B}{(3B)^{2/3}}} = \sqrt{1 - 16^3 \sqrt{\frac{B}{9}}} \quad (32)$$

$$B = \frac{\tau_0 L}{\rho \cdot g \cdot H^2} = \frac{\tau_0 \times 0.1}{\rho \cdot g \times 0.6^2} = \frac{5\tau_0}{18\rho \cdot g} \quad (33)$$

So finally we have:

$$B = \frac{5\tau_0}{18\rho \cdot g} \quad (34)$$

$$\frac{H_2}{H_1} = \sqrt{1 - 5.0189 \times \sqrt[3]{\frac{\tau_0}{\rho \cdot g}}} \quad (35)$$

Solving Eq. 35 for  $\tau_0$  results in:

$$\tau_0 = 0.0079 \rho \cdot g \cdot \left(1 - \left(\frac{H_2}{H_1}\right)^2\right)^3 \quad (36)$$

A plot of Eq. 36 for different values of  $\frac{H_2}{H_1}$  is shown in Fig. 3.

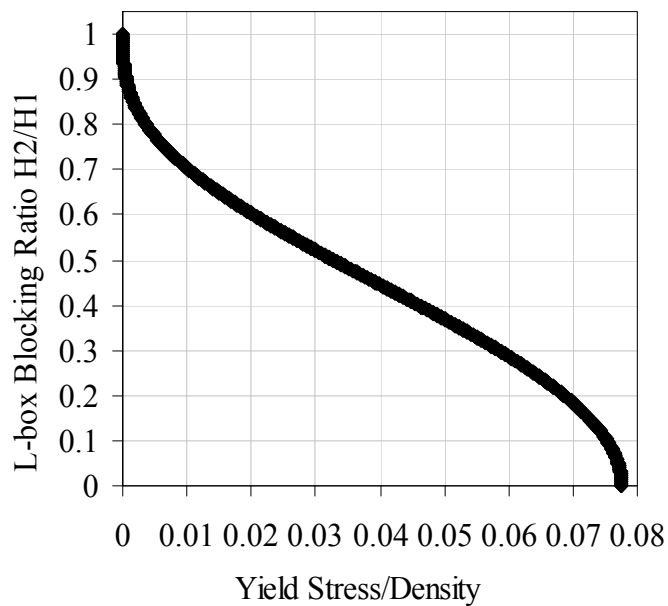


Fig.3 Plot of Eq. 36 for Different Values of  $\frac{H_2}{H_1}$

## COMPARISON OF MODELS

The proposed numerical dam-break model has been validated against a number of benchmark test cases widely documented in the literature. Three test cases are considered<sup>9, 10, and 12</sup>. The difference between the present model and Nguyen et al.<sup>6</sup> model has been compared by inserting the test results. The following steps are used to compare the models and test data.

Step1: The yield stress ( $\tau_0$ ) in Eqs. 8 and 35, are substituted by the experimental measured data.

Step2: The ratios  $\frac{H_2}{H_1}$  are calculated from two models, and they are compared with the experimental measured data.

Step3: The ratio  $\frac{H_2}{H_1}$  in Eqs. 9 and 36, are substituted by the experimental measured data.

Step4: The yield stresses ( $\tau_0$ ) are calculated from two models, and they are compared with the experimental measured data.

It must be noted that the densities,  $\rho$ , of experimental mixtures obtained from literature are approximately  $2500 \text{ kg/m}^3$ . For this value of density Eq. 8 is valid for  $\tau_0 \leq 197.1 \text{ Pa}$  and Eq. 35 is valid for  $\tau_0 \leq 194 \text{ Pa}$ .

Computational results were compared to the experimental data obtained by Petersson et al.<sup>9</sup> and presented in Table 1. Results illustrate that the predicted values obtained with proposed dam-break model are in good agreement with the experimental data.

Table.1 Comparison Between Petersson et al.<sup>9</sup> Data and the Results from Dam-Break Model and Nguyen et al.<sup>6</sup> Model

	Experimental yield stress $\tau_0$ (Pa)	$\frac{H_2}{H_1}$ Nguyen et al. <sup>6</sup> model	$\frac{H_2}{H_1}$ Dam-break model	Experimental $\frac{H_2}{H_1}$
	0	1	1	0.89
	13.7	0.870	0.766	0.31
<b>Steps 1 and 2</b>	32.8	0.715	0.669	1
	43.6	0.638	0.626	0.87
	34.6	0.701	0.661	0.65
	107.4	0.295	0.423	0.58
	109.6	0.285	0.416	0.37
	216.4	-	-	0.23
	245.9	-	-	0.17
	259.7	-	-	0.04
	Experimental $\frac{H_2}{H_1}$	Nguyen et al. <sup>6</sup> yield stress $\tau_0$ (Pa) model	Dam-break yield stress $\tau_0$ (Pa) model	Experimental yield stress $\tau_0$ (Pa)
	0.89	11.470	1.741	0
	0.31	103.803	143.086	13.7
<b>Steps 3 and 4</b>	1	0	0	32.8
	0.87	13.700	2.783	43.6
	0.65	41.804	37.316	34.6
	0.58	52.387	56.618	107.4
	0.37	90.626	124.572	109.6
	0.23	123.373	164.598	216.4
	0.17	139.806	177.430	245.9
	0.04	181.916	192.819	259.7

Emborg<sup>10</sup> reported experimental L-box blocking ratio ( $\frac{H_2}{H_1}$ ), but note that the values of yield stress ( $\tau_0$ ) in this paper are in the form of g (N.m). According to information mentioned in the report ‘Comparison of concrete rheometers, provided by The United States National Institute of Standards and Technology (NIST)<sup>11</sup>, these values can be turned into  $\tau_0$  (Pa) through the following equation:

$$\tau_0(Pa) = 122g \quad (37)$$

Experimental data from Emborg<sup>10</sup> together with results of the two models are provided in Table 2. A comparison between the data and the results of two models illustrate that the dam-break model is in a fairly good agreement with the measured data.

Table.2 Comparison Between Emborg<sup>10</sup> Data and the Results from Dam-Break Model and Nguyen et al.<sup>6</sup> Model

	Experimental yield stress $\tau_0$ (Pa)	$\frac{H_2}{H_1}$ Nguyen et al. <sup>6</sup> model	$\frac{H_2}{H_1}$ Dam-break model	Experimental $\frac{H_2}{H_1}$
<b>Steps 1 and 2</b>	3.66	0.964	0.857	0.8
	5.002	0.950	0.839	0.73
	11.102	0.893	0.784	0.63
	27.084	0.758	0.694	0.58
	28.304	0.749	0.688	0.62
	31.842	0.722	0.673	0.76
	37.82	0.678	0.6482	0.89
	39.04	0.669	0.643	0.76
	48.8	0.603	0.607	0.69
	56.242	0.556	0.582	0.72
	58.682	0.541	0.573	0.8
	74.786	0.450	0.522	0.63
	75.64	0.445	0.519	0.625
		Experimental $\frac{H_2}{H_1}$	Nguyen et al. <sup>6</sup> yield stress $\tau_0$ (Pa) model	Dam-break yield stress $\tau_0$ (Pa) model
<b>Steps 3 and 4</b>	0.8	21.897	9.039	3.66
	0.73	30.758	19.7454	5.002
	0.63	44.735	42.501	11.102
	0.58	52.387	56.618	27.084
	0.62	46.228	45.199	28.304
	0.76	26.874	14.602	31.842
	0.89	11.470	1.741	37.82
	0.76	26.874	14.602	39.04
	0.69	36.150	27.860	48.8
	0.72	32.082	21.642	56.242
	0.8	21.897	9.039	58.682
	0.63	44.735	42.501	74.786
	0.625	45.479	43.842	75.64

Experimental data from Sonebi<sup>12</sup> together with results of the two models are provided in Table 3. It must be noted that in this paper similar to the previous one, the values of yield stress are presented in the form of  $g$  (N.m) and can be transformed into  $\tau_0$  (Pa) by using Eq. 37.

A comparison between the data and the results of two models illustrate that when substituting the yield stress ( $\tau_0$ ) in Eqs. 8 and 35 by experimental measured data, two models can not present any answer for theoretical L-box blocking ratio ( $\frac{H_2}{H_1}$ ), but in the case of theoretical yield stress ( $\tau_0$ ), a comparison between the data and the results of two models illustrate that the dam-break model is in a better agreement with the measured data.

Experimental data from three mentioned paper accompanied by results of the two models are shown in Fig. 4 and Fig. 5.

Table.3 Comparison Sonebi<sup>12</sup> Data and the Results from Dam-Break Model and Nguyen et al.<sup>6</sup> Model

	Experimental yield stress $\tau_0$ (Pa)	$\frac{H_2}{H_1}$ Nguyen et al. <sup>6</sup> model	$\frac{H_2}{H_1}$ Dam-break model	Experimental $\frac{H_2}{H_1}$
<b>Steps 1 and 2</b>	564.86	-	-	0
	318.42	-	-	0.45
	242.78	-	-	0.43
	315.98	-	-	0.2
	450.18	-	-	0
	215.94	-	-	0.31
	273.28	-	-	0.45
	204.96	-	-	0.32
	219.6	-	-	0
	214.72	-	-	0.41
	313.54	-	-	0
	Experimental $\frac{H_2}{H_1}$	Nguyen et al. <sup>6</sup> yield stress $\tau_0$ (Pa) model	Dam-break yield stress $\tau_0$ (Pa) model	Experimental yield stress $\tau_0$ (Pa)
<b>Steps 3 and 4</b>	0	197.076	193.748	564.86
	0.45	74.753	98.272	318.42
	0.43	78.555	104.923	242.78
	0.2	131.384	171.415	315.98
	0	197.076	193.748	450.18
	0.31	103.803	143.086	215.94
	0.45	74.753	98.272	273.28
	0.32	101.524	140.115	204.96
	0	197.076	193.748	219.6
	0.41	82.464	111.545	214.72
	0	197.076	193.748	313.54

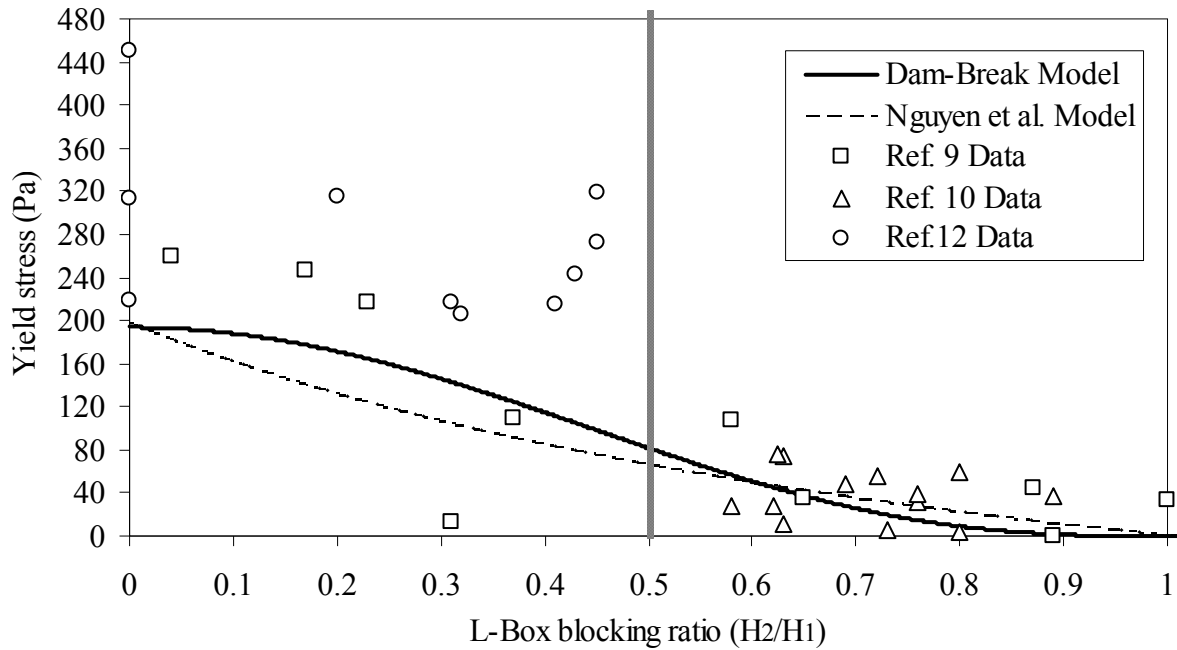


Fig.4 Comparison Between the Values of Yield Stress Obtained from the Dam-Break Model and Nguyen et al.<sup>6</sup> Model for the Measured Values of  $\frac{H_2}{H_1}$  in L-Box Test

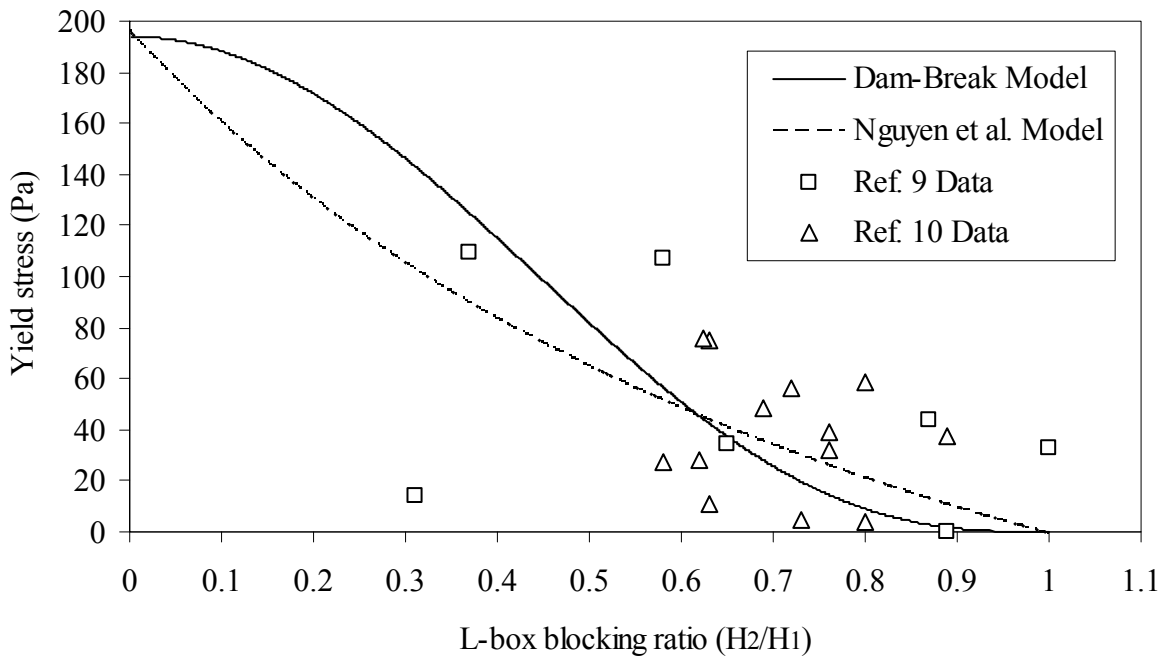


Fig.5 Comparison Between Values of  $\frac{H_2}{H_1}$  Obtained from Dam-Break Model and Nguyen et al.<sup>6</sup> Model for the Yield Stresses Measured by Viscometer

Correlation between experimental and calculated yield stress and also L-box Blocking Ratio ( $\frac{H_2}{H_1}$ ) are shown in Figs. 6 and 7 respectively.

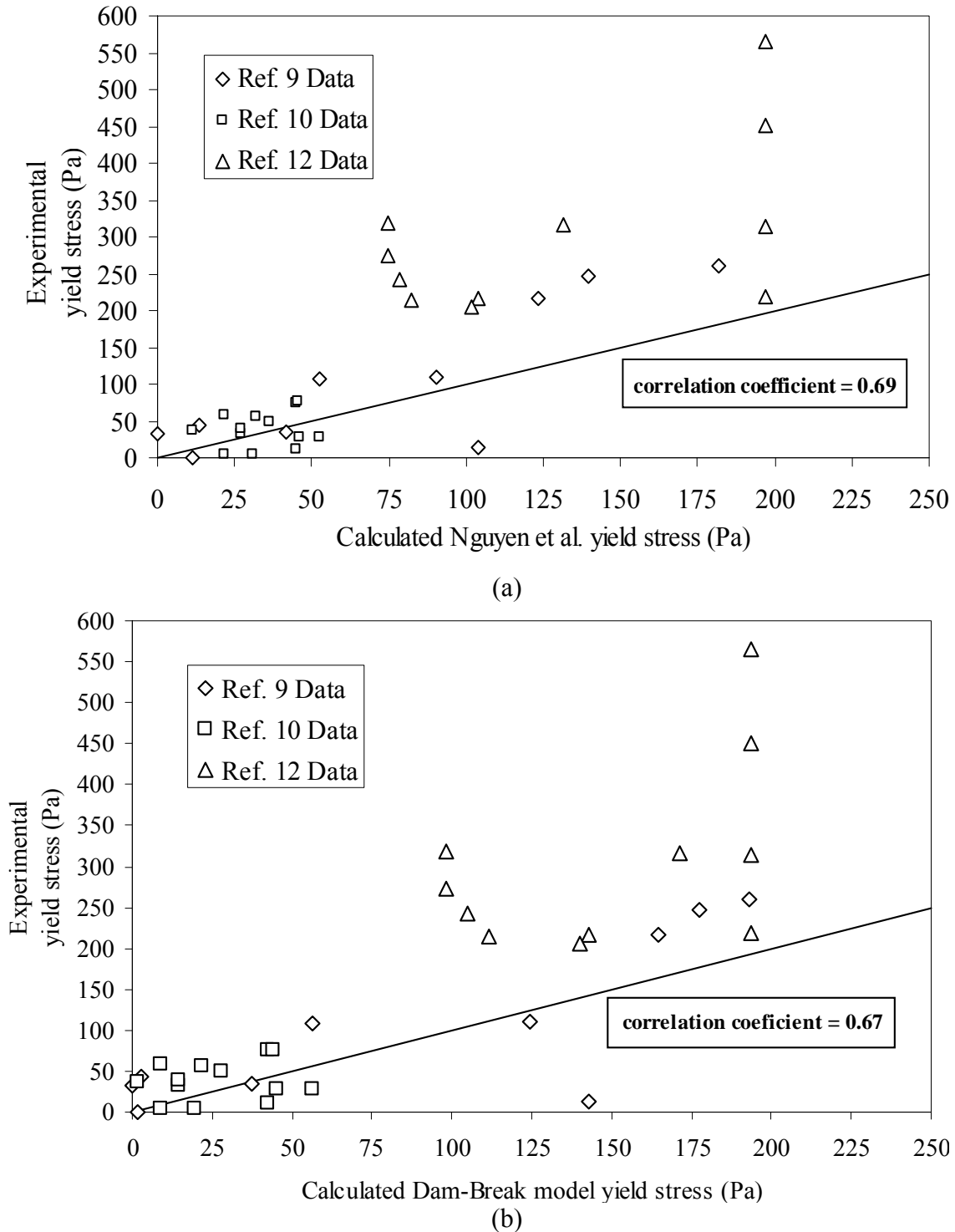
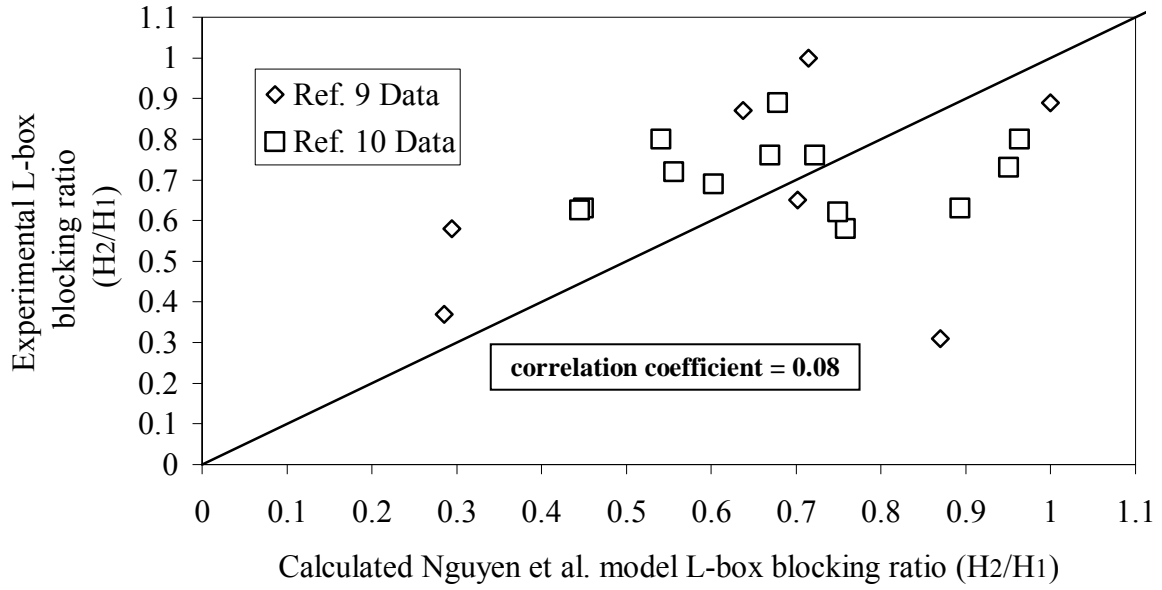
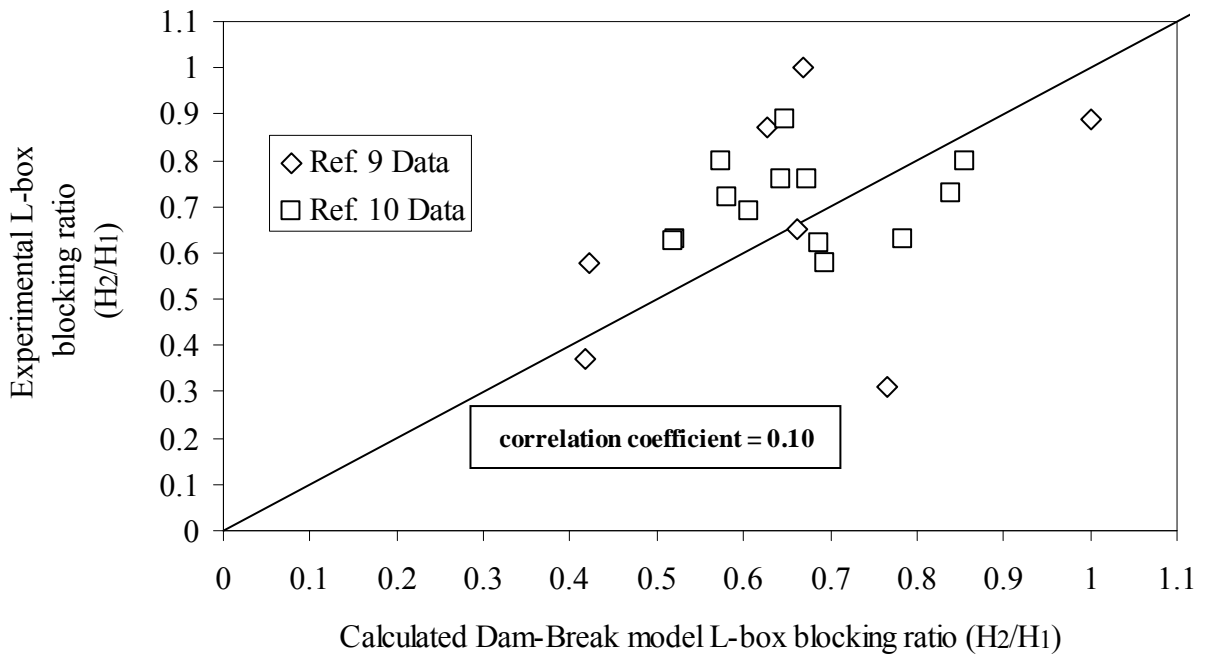


Fig. 6 Correlation Between Experimental and Calculated Yield Stress



(a)



(b)

Fig. 7 Correlation Between Experimental and Calculated L-box Blocking Ratio ( $\frac{H_2}{H_1}$ )

## RESULTS AND DISSCUSION

Observations fall into two different categories. First one is the comparison between the derived results of yield stress from the models and the experimental data. The second one is the comparison of blocking ratios obtained from the models and the experimental ratios. We discuss each case separately.

### a) COMPARISON OF YIELD STRESSES

Observing Fig. 4 turns out that these diagrams have three distinct parts as:

Part 1: Yield stress between 0 and 30 Pa; in this part both models give almost the same value. However, it seems that the model that was derived using dam break phenomenon has a relative superiority over Nguyen et al.<sup>6</sup> model and its predicted values are closer to the experimental ones.

Part 2: Yield stress between 30 and 50 Pa; in this part, the predicted values of both models are nearly the same and have an analogous order of accuracy.

Part 3: Yield stress more than 50 Pa; in this part it is obviously observed that the model obtained from dam break problem evaluates the values of yield stress more precise than that of Nguyen et al.<sup>6</sup> model, so experimental data seem to correlate quite well with dam-break model.

In addition, it can be seen that both models underestimate the yield stress for  $\frac{H_2}{H_1}$  values less than about 0.50. It mainly occurs due to the fact that in this range of  $\frac{H_2}{H_1}$  the potential of SCC for segregation and blocking increase resulting in the invalidity of the fundamental assumption of the homogeneity of fluid. Anyway, this range of  $\frac{H_2}{H_1}$  is not desirable for SCC considering that it is recommended to be 0.6 to 0.8 by various researchers<sup>13</sup>.

### b) COMPARISON BETWEEN $\frac{H_2}{H_1}$ RATIOS

Observing Fig. 5 yield that these diagrams can also be divided into two distinct parts as:

Part 1: Yield stress between 0 and 40 Pa; in this part, Nguyen et al.<sup>6</sup> model predicts higher values of yield stress in comparison with the model presented in this work. How ever, the presented model gives better values in this zone.

Part 2: Yield stress more than 40 Pa; in this part, the presented dam-break model gives higher values of yield stress in comparison with the model proposed by Nguyen et al.<sup>6</sup>. Similarly, the presented dam-break model evaluates better values in this zone.

As it is observed from Figs. 6 and 7, for both models the evaluation of yield stress ( $\tau_0$ ) and L-box blocking ratio ( $\frac{H_2}{H_1}$ ) almost fall in the same range. In the case of yield stress the correlation coefficient between experimental and calculated data is of acceptable order. However, for blocking ratio neither of the models gives a reliable prediction.

## CONCLUSIONS

In order to study the relationship between the flow characteristics of L-box test, a new numerical model has been proposed. This model which is derived from theory of dam-break phenomenon, is more accurate than Nguyen et al.<sup>6</sup> model for prediction yield stress and L-box blocking ratio ( $\frac{H_2}{H_1}$ ) in the range of 0-75 Pa and 0.55-1 respectively. Since these ranges are recommended for SCC in the literature, hence the proposed model is appropriate for SCC.

## REFERENCES

1. Rols, S., Amboise, J., and Pera, J., "Effects of different viscosity agents on the properties of Self-Leveling concrete," *Cement and Concrete Research*, V.29, No.2, 1999, pp. 261-266.
2. Khayat, K.H., Hu, C., and Monty, H., "Stability of Self-Consolidating Concrete, advantages and potential application," *Proc. Of the 1st International RILEM Symposium on Self Compacting Concrete, Editors: Skarendahl, A. and Petersson, O., Stockholm, Sweden, September 13-14, 1999*, pp. 143-152.
3. Saak, A., Hamlin, M.J., and Shah, S.P., "Characterization of the rheological properties of cement pastes for use in self-compacting concrete," *Proc. Of the 1st International RILEM Symposium on Self Compacting Concrete, Editors: Skarendahl, A. and Petersson, O., Stockholm, Sweden, September 13-14, 1999*, pp. 83-94.
4. Schwartzentruber, L.D'A., Leroy, R., and Cordin, J., "Rheological behaviour of fresh cement pastes formulated from a Self Compacting Concrete (SCC)," *Cement and Concrete Research*, V.36, 2006, pp. 1203-1213.
5. Saak, A.W., Jennings, H.M., and Shah, S.P., "A generalized approach for the determination of yield stress by slump and slump flow," *Cement and Concrete Research*, V.34, 2004, pp. 363-371.
6. Nguyen, T.L.H., Roussel, N., and Coussot, P., "Correlation between L-box test and rheological parameters of a homogeneous yield stress fluid," *Cement and Concrete Research*, V.36, 2006, pp. 1789-1796.

7. Matson, G.P., Hog, A.J., “Two-dimensional dam break flows of Herschel–Bulkley fluids: The approach to the arrested state,” *J. Non-Newtonian Fluids Mech*, V.142, 2007, pp. 79-94.
8. Balmforth, N.J., Craster, R.V., Perona, P., Rust, A.C., and Sassi, R., “Viscoplastic dam breaks and the Bostwick consistometer,” *J. Non-Newtonian Fluids Mech*, V.142, 2007, pp. 63-78.
9. Petersson, O., and Billberg, P., “Investigation on Blocking of Self Compacting Concrete with Different Maximum Aggregate size and Use of Viscosity Agent Instead of Filler,” *Proc. Of the 1st International RILEM Symposium on Self Compacting Concrete, Editors: Skarendahl, A. and Petersson, O., Stockholm, Sweden, September 13-14, 1999*, pp. 333-344.
10. Emborg, M., “Rheology Tests for Self-Compacting-Concrete How Useful Are They for the Design of Concrete Mix for Full Scale Production?,” *Proc. Of the 1st International RILEM Symposium on Self Compacting Concrete, Editors: Skarendahl, A. and Petersson, O., Stockholm, Sweden, September 13-14, 1999*, pp. 95-105.
11. “Comparison of concrete rheometers,” International tests at MB (Cleveland OH, USA), May 2003, *National Institute of Standards and Technology (NIST)*, Page 23
12. Sonebi, M., “Medium strength self-compacting concrete containing fly ash: Modelling using factorial experimental plans,” *Cement and Concrete Research*, V.34, 2004, pp. 1199-1208.
13. Pedersen, B., and Mortsell, E., “Characterization of fillers for SCC,” *Proc. of the Second International Symposium on Self-Compacting Concrete, Tokyo, Japan, 2001*, pp. 257-266.